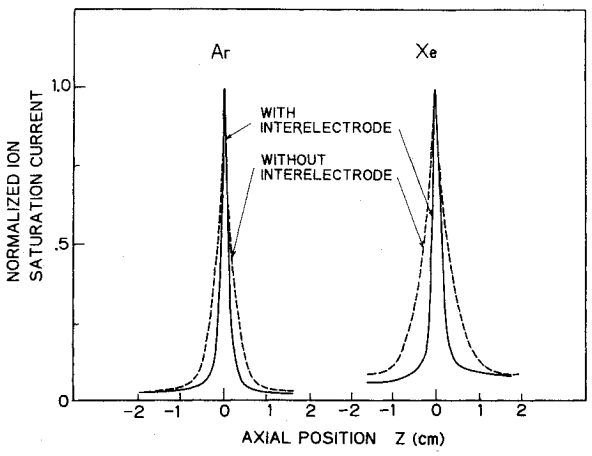

Fig. 2 Density distributions of ion saturation currents for argon and xenon plasmas at $\dot{m} = 1$ A, $V_d = 40$ V, $I_d = 5$ A.

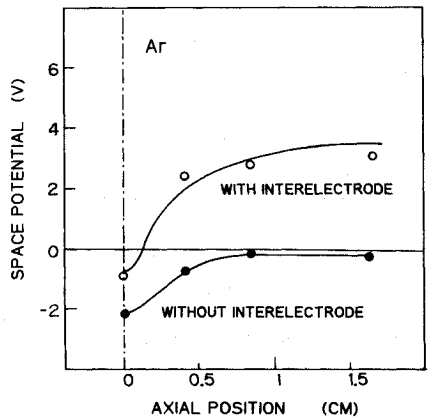

Fig. 3 Spatial potential distributions at the wall surface with and without interelectrodes.

Figure 3 shows the axial distribution of the space potential at the wall surface (expressed in values relative to the space potential at the chamber axis) operated with and without interelectrodes for the same operating condition as seen in Fig. 2 ($\dot{m} = 1$ A, $V_d = 40$ V, $I_d = 5$ A). This result was obtained from the emitting probe that was scanned on the same trace as the previous density measurement. The potential valley is seen at the center of the cusp for operations both with and without interelectrode. This fact may be explained as follows. The electron generated in the field-free region hardly penetrates into the intercusp region traveling across the magnetic field lines because of its extremely small Larmor radius (0.1 mm), while the ion can easily penetrate the region. This situation produces a strong space charge electric field that ensures charge neutrality.[6] Although the space potential is negative at any axial position without an interelectrode, it turns out to be positive except at the region around the center of the cusp with an interelectrode. At present, we do not have information to explain the mechanism of this potential rise, but it may be considered that electrons, magnetically trapped in the intercusp region, are collected and absorbed into the positively biased interelectrodes, thus raising the space potential in the intercusp region. In this situation, the plasma ions escaping from the field-free region will experience a repulsive electrostatic force and be reflected back before reaching the wall surface, resulting in the reduction of the ions lost at the walls after passing through the intercusp region.

Figure 4 is a plot of the rate of increase of the ion density averaged over the screen grid surface ($\Delta N_i/N_i$) as a function of the fraction of the additional power supplied to the interelectrodes to the discharge power ($\Delta P/P$). The ion density

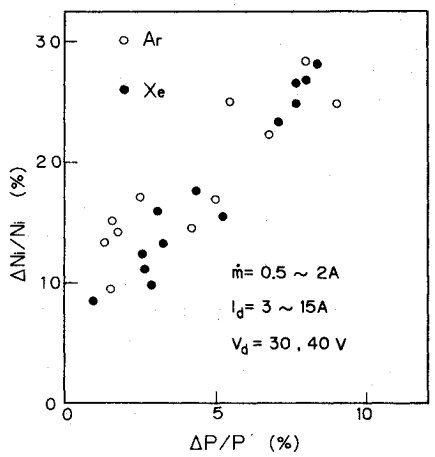

Fig. 4 The rate of the increase in ion density as a function of the fraction of the additional power to the discharge power.

increases almost linearly with the additional power and its rate is independent of discharge parameters such as the discharge current, propellant type, and propellant flow rate. About a 30% increase of the ion density can be attained when only 8% of the electric power is added to the discharge chamber. This result indicates that the installation of the interelectrodes is an effective method for reducing the ion loss to the chamber walls and improving the discharge performance.

References

[1]Brophy, J. R. and Wilbur, P. J., "Simple Performance Model for Ring and Line Cusp Ion Thrusters," *AIAA Journal,* Vol. 23, Nov. 1985, pp, 1731-1736.

[2]Sovey, J. S., "Improved Ion Containment Using a Ring-Cusp Ion Thruster," *Journal of Spacecraft and Rockets,* Vol. 21, May 1984, pp. 488-495.

[3]Arakawa, Y., Hamatani, C., and Kawasaki, Y., "Wall Losses of Charged Particles in a Multipole Discharge Plasma," IEPC Paper 84-69, 1984.

[4]Makowski, M. A. and Emmert, G. A., "New Method to Measure Plasma Potential with Emissive Probes," *Review of Scientific Instruments,* Vol. 57, July 1983, pp. 830-836.

[5]Leung, K. N., Hershkowitz, N., and Mackenzie, K. R., "Plasma Confinement by Localized Cusps," *The Physics of Fluids,* Vol. 19, July 1976, pp. 1045-1053.

[6]Marcus, A. J., Knorr, G., and Joyce, G., "Two-Dimensional Simulation of Cusp Confinement of a Plasma," *Plasma Physics,* Vol. 22, 1980, pp. 1015-1027.

Off-Design Analysis of Counter-Rotating Propeller Configurations

K. D. Korkan* and J. A. Gazzaniga†
Texas A&M University, College Station, Texas

Introduction

In a recent investigation, Playle et al.[1] and Korkan and Playle[2] conducted studies to develop a theoretical method by which counter-rotating propellers could be designed and

Received May 13, 1981; revision received Aug. 8, 1986.

*Associate Professor, Aerospace Engineering Department. Associate Fellow AIAA.

†Graduate Research Assistant, Aerospace Engineering Department. Student Member AIAA.

analyzed. The method of Davidson[3] was selected because his theoretical approach yielded realistic designs of planform and performance values of counter-rotating propeller configurations and was adaptable to further development. Playle et al. included drag and compressibility in their study and investigated the off-design analysis of counter-rotating propeller configurations at a fixed-pitch condition. Playle's study of the off-design condition yielded a very broad and flat efficiency map for a large variance of advance ratio J and emphasized the usefulness of the counter-rotating propeller configuration. In this previous study, the variation in J was obtained by holding the freestream velocity and twist distribution constant and varying the rpm of both the front and back propeller disks, keeping equal rpm values for both disks.

In the present study, an analysis has been conducted to determine whether the counter-rotating propeller configuration maintains and possibly improves its excellent performance characteristics in the off-design mode for the constant-speed or variable-pitch case. Here, the twist distribution is maintained and the blade angle is changed to absorb the shaft horsepower, while holding constant rpm under varying freestream velocities.

Analysis

Using the design segment of the method of Playle et al., the planform and twist distribution for the front and aft propeller(s) were obtained. The design condition chosen consisted of a freestream velocity of 625 ft/s at 28,000 ft altitude using two powerplants of 900 shp each. The four blade front/aft propeller geometrical values given in Fig. 1 were determined by assuming a propeller thickness-to-chord distribution, utilization of a NACA four-digit airfoil data bank, a front/aft propeller diameter of 7.5 ft, and a design lift coefficient radial distribution CL_D that resulted in an integrated lift coefficient CL_i of 0.522.

The off-design segment of the method of Playle et al. allows the investigation of the off-design performance of counter-rotating propeller configurations. In the present study, this off-design mode was utilized by varying the freestream velocity about the design point and holding the rpm at 1500 to obtain a range of advance ratios J of 1.2–4.8. Advance ratio is defined as V_∞/nD, where V_∞ is the freestream velocity, n the revolutions per second, and D the diameter of the propeller. The previous study[1] had been accomplished for a fixed-pitch configuration; however, the present analysis allows a variable-pitch or constant-speed condition where the twist distribution is incremented to match the power coefficient C_p based on the aerodynamic values of torque to that of the 900 shp of each powerplant. The resulting twist angle of the front/aft counter-rotating propeller configuration at the 75% radial location is shown in Fig. 2 as a function of the advance ratio J. As noted in this figure, as the freestream velocity is decreased to obtain the lower J values, the twist angle is increased to increase the angle of attack (and hence drag and torque) to match the on-power coefficient for the constant-speed case. This result may be examined by observation of the angle-of-attack variation at the 75% radial location for the range of advance ratios given in Fig. 3. Here, the angle of attack at this radial location is approximately equal for the front/aft propeller disks and appears to be in a reasonable range up to a J value of approximately 1.5. The NACA four-digit airfoil data bank utilized in this study does contain maximum lift coefficient values, which are utilized at the low J values contained in study.

The thrust coefficient C_T performance values for the counter-rotating propeller configuration for this study is shown in Fig. 4. The variation of C_T with J increases over the advance ratios of interest to a J of approximately 1.5, with the C_T value for the back propeller disk being significantly larger than the front disk due to the swirl velocity component. As noted, at a J value of approximately 1.5, the C_T values decrease as a result of the high angle of attack at each radial location, i.e., the maximum lift coefficient boundary of the

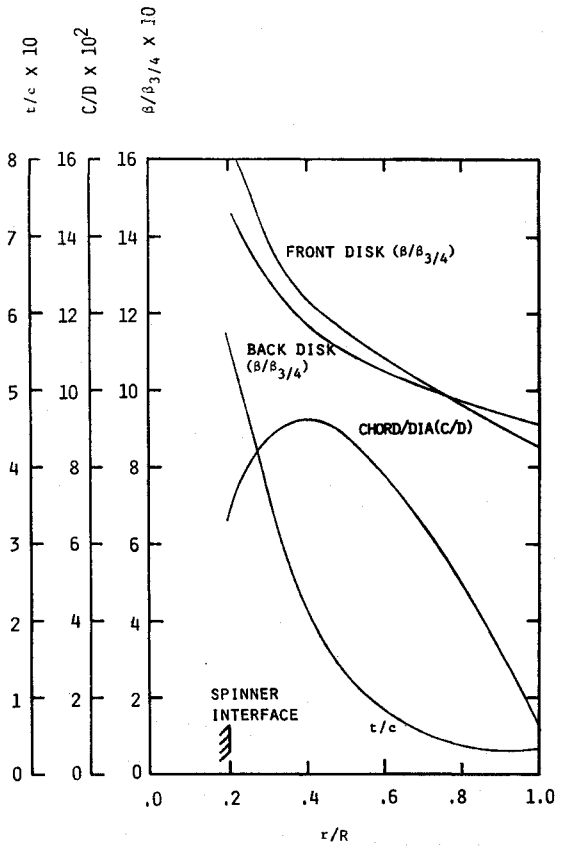

Fig. 1 Geometrical characteristics of front/aft counter-rotating propeller configuration (t/c = maximum thickness-to-chord ratio, c/D = chord-to-diameter ratio, $\beta/\beta_{3/4}$ = twist angle to twist angle at ¾ R).

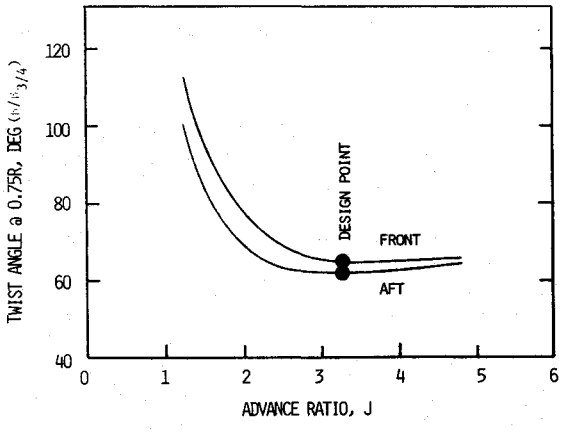

Fig. 2 Twist angle of front/aft propeller(s) at 75% radial location in off-design mode (rpm = 1500).

airfoil(s) contained in the propeller(s) is exceeded. The power coefficient C_p variation with advance ratio, as anticipated, is an equal value for the front/aft propeller disk and constant as a function of J due to the condition of constant speed, unlike that of Playle et al.[1] Examination of the propeller efficiency η as a function of advance ratio yields the variation shown in Fig. 5, where η is defined as $(C_T/C_p)J$. The interaction in terms of swirl velocities due to the front/aft propeller disks results in a broadening of the η vs J performance envelope about the design point. This result indicates that the counter-rotating propeller configuration improves the performance of rotating systems significantly, not only in the cruise condition with propeller efficiency in excess of 90%, but also maintains this level during the takeoff and climb condition.

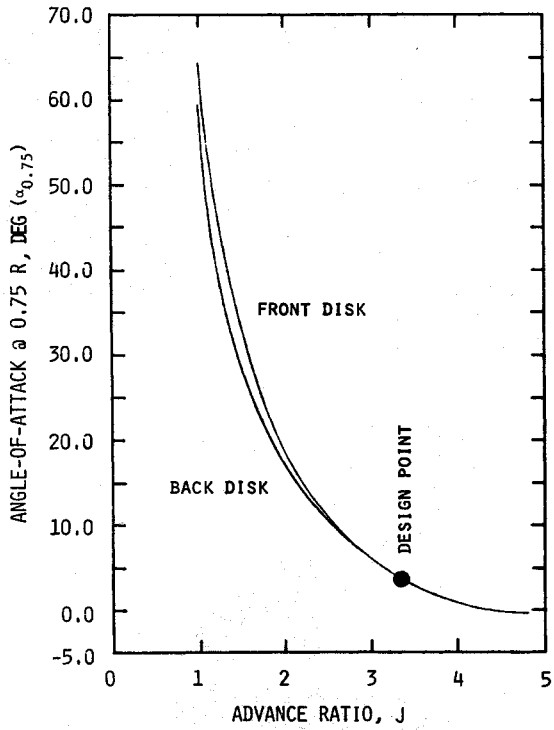

Fig. 3 Angle of attack of front/aft propeller(s) at 75% radial location as function of advance ratio.

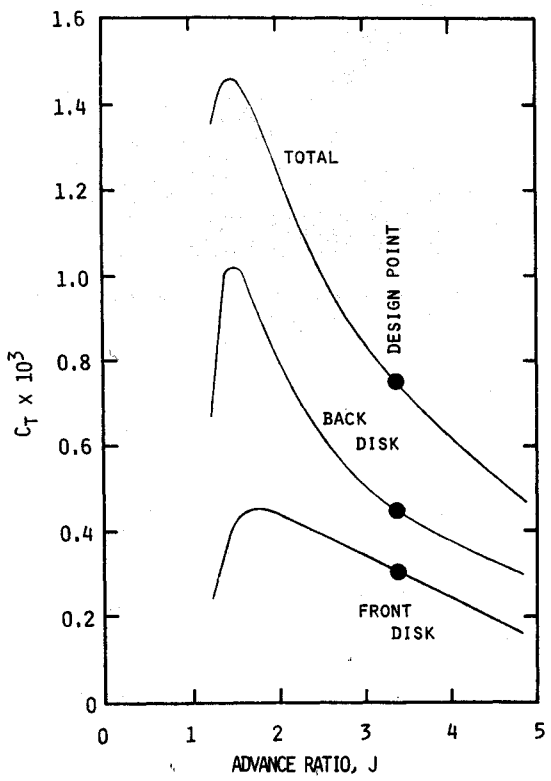

Fig. 4 Thrust coefficients of front/aft propeller(s) as function of advance ratio for off-design mode.

Summary

Using the method of Playle et al., as given by Davidson, the off-design performance of counter-rotating propeller configurations has been investigated. As in Playle's original study for the fixed-pitch condition, the off-design analysis for a variable-pitch or constant-speed condition of the counter-rotating propeller yielded a relatively flat propeller efficiency

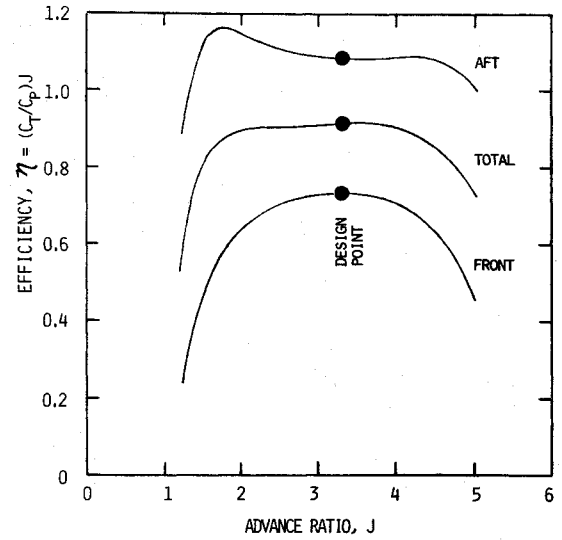

Fig. 5 Propeller efficiency of counter-rotating propeller configuration in off-design mode.

curve for advance ratios of 1.5–5. This type of performance has again indicated the full extent of the performance advantages of counter-rotating propeller configurations when analyzed for off-design conditions.

Acknowledgment

This research was supported by the NASA Lewis Research Center, Grant NAG 3-354.

References

[1]Playle, S. C., Korkan, K. D., and von Lavante, E., "A Numerical Method for the Design and Analysis of Counter-Rotating Propellers," *Journal of Propulsion and Power*, Vol. 2, Jan.-Feb. 1986, pp. 57–63.

[2]Korkan, K. D., "On the Design of Counterrotating Propellers," SAE Paper 830773, April 1983.

[3]Davidson, R. E., "Optimization and Performance Calculation of Dual-Rotation Propellers," NASA TP 1948, Dec. 1981.

Flow Generated by Ramp Tabs in a Rocket Nozzle Exhaust

J. M. Simmons,* C. M. Gourlay,† and B. A. Leslie†
University of Queensland
Brisbane, Queensland, Australia

Introduction

MANY schemes have been studied for thrust vector control of rockets. The usual aim is to obtain control of the direction of the thrust vector while minimizing unwanted reduction of its magnitude. Reported here is a study of a scheme in which three ramp tabs can be partially inserted into the nozzle exhaust at large angles to the flow, thereby

Presented as Paper 86-0282 at the AIAA 24th Aerospace Sciences Meeting, Reno, NV, Jan. 6–9, 1986; received May 2, 1986.

*Reader, Mechanical Engineering. Member AIAA.
†Research Student, Mechanical Engineering.